

A solid state light-matter interface at the single photon level

Hugues de Riedmatten *, Mikael Afzelius *, Matthias U. Staudt, Christoph Simon, and Nicolas Gisin
Group of Applied Physics, University of Geneva, CH-1211 Geneva 4, Switzerland

Coherent and reversible mapping of quantum information between light and matter is an important experimental challenge in quantum information science. In particular, it is a decisive milestone for the implementation of quantum networks and quantum repeaters [1, 2, 3]. So far, quantum interfaces between light and atoms have been demonstrated with atomic gases [4, 5, 6, 7, 8, 9], and with single trapped atoms in cavities [10]. Here we demonstrate the coherent and reversible mapping of a light field with less than one photon per pulse onto an ensemble of $\sim 10^7$ atoms naturally trapped in a solid. This is achieved by coherently absorbing the light field in a suitably prepared solid state atomic medium [11]. The state of the light is mapped onto collective atomic excitations on an optical transition and stored for a pre-programmed time up to $1\mu\text{s}$ before being released in a well defined spatio-temporal mode as a result of a collective interference. The coherence of the process is verified by performing an interference experiment with two stored weak pulses with a variable phase relation. Visibilities of more than 95% are obtained, which demonstrates the high coherence of the mapping process at the single photon level. In addition, we show experimentally that our interface allows one to store and retrieve light fields in multiple temporal modes. Our results represent the first observation of collective enhancement at the single photon level in a solid and open the way to multimode solid state quantum memories as a promising alternative to atomic gases.

Efficient and reversible mapping of quantum states between light and matter requires strong interactions between photons and atoms. With single quantum systems, this regime can be reached with high finesse optical cavities, which is technically highly demanding [10]. In contrast, light can be efficiently absorbed in ensembles of atoms in free space. Moreover, it is possible to engineer the atomic systems such that the stored light can be retrieved in a well defined spatio-temporal mode due to a collective constructive interference between all the emitters. This collective enhancement is at the heart of protocols for storing photonic quantum states in atomic ensembles, such as schemes based on Electromagnetically-Induced Transparency (EIT)[12], off-resonant Raman interactions [2, 13] and modified photon echoes using Controlled Reversible Inhomogeneous Broadening (CRIB)[14, 15, 16] and Atomic Frequency Combs (AFC) [11].

All previous quantum storage experiments with ensembles have been performed using atomic gases as the storage material [4, 5, 6, 7, 8, 9]. However, some solid state systems have properties that make them very attractive for applications in quantum storage. In particular, rare-earth ion doped solids provide a unique physical system where large ensembles of atoms are naturally trapped in a solid state matrix, which prevents decoherence due to the motion of the atoms and allows the use of trapping free protocols. Moreover, these systems also exhibit excellent coherence properties at low temperature (below 4 K), both for the optical [17] and spin transition [18]. The long optical coherence

times enable storage of multiple temporal modes in a single QM, which promises significant speed-up in quantum repeater applications[3]. Furthermore, high optical densities can be obtained in rare-earth doped solids, which is required to achieve strong light matter coupling resulting in high efficiency light storage and retrieval. However, despite recent experimental progress [19, 20, 21, 22, 23, 24], the implementation of a solid state light matter quantum interface has not been reported so far.

Here we demonstrate for the first time the coherent and reversible mapping of weak coherent states of light with less than one photon per pulse onto a large number of atoms in a solid. The mapping is done by coherently absorbing the light in an ensemble of inhomogeneously broadened atoms spectrally prepared with a periodic modulation of the absorption profile [11, 25, 26, 27]. The reversible absorption by such a spectral grating is at the heart of the recently proposed multimode quantum memory scheme based on AFC [11]. We therefore also demonstrate a proof of principle of an essential primitive of this protocol at the single photon level.

Let us now describe in more detail how our interface works. Assume an incident weak coherent state of light $|\alpha\rangle_L$ with a mean photon number $\bar{n} = |\alpha|^2 < 1$. After absorption the photons are stored in a coherent superposition of collective optical excitations de-localized over all the atoms in resonance with the light field. The state of the atoms (not normalized) can be written as:

$$|\alpha\rangle_A = |0\rangle_A + \alpha|1\rangle_A + O(\alpha^2) \quad (1)$$

where $|0\rangle_A = |g_1 \cdots g_N\rangle$ and

* These authors contributed equally to this work.

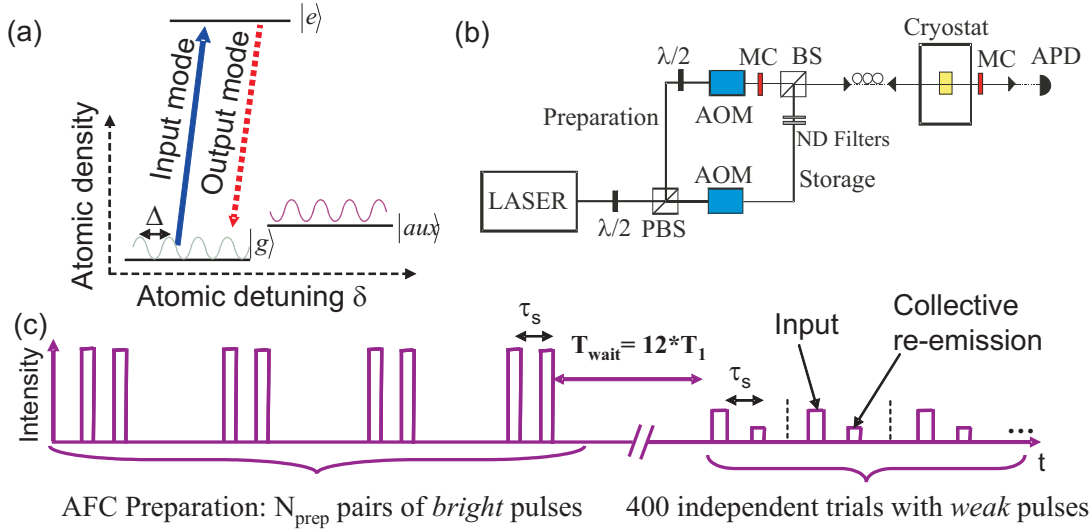


FIG. 1: (a) Solid state light matter interface. The light is absorbed on the ${}^4I_{9/2} \rightarrow {}^4F_{3/2}$ transition of Nd^{3+} ions at 880 nm. The inhomogeneous broadening of the optical transition is 2 GHz, with a maximal optical depth around 4. The optical relaxation time T_1 of the excited state $|e\rangle$ is equal to $100 \mu\text{s}$. The ground state is split into two Zeeman levels $|g\rangle$ and $|aux\rangle$, separated by 3.8 GHz through the application of a magnetic field of 300 mT. A spectral grating is prepared in $|g\rangle$ by a preparation sequence described in the Methods section. (b) Experimental setup. The laser source is a cw external cavity diode laser at 880 nm. The laser is split at a variable beam splitter and the pulse sequences for the preparation of the grating and for the pulses to be stored are prepared by independent acousto-optics modulators in different optical paths. The duration of the pulses is about 30 ns. These paths are then recombined at a beam splitter (BS) and coupled into a single mode fiber to ensure proper mode matching. The light is then focussed onto 1 mm long $\text{Nd}^{3+}:\text{YVO}_4$ crystal with a beam diameter of $30 \mu\text{m}$. The crystal is cooled down to 3 K by a pulse tube cooler. After the sample, the light passes through a polarizer and is coupled back to a single mode fiber, which is connected to a Silicon Avalanche Photo diode single photon counter. In order to block the preparation light during the storage and to protect the detector from the intense preparation light, two mechanical choppers (MC) are used. (c) Optical pulse sequence. The experimental sequence is divided into two parts: the preparation of the spectral grating (see Methods) and the storage of the weak pulses. We wait a time $T_w = 12T_1 = 1200 \mu\text{s}$ between the preparation and the storage sequence in order to avoid fluorescence. During the storage sequence, 400 independent trials are performed at a repetition rate of 200 kHz. The entire sequence preparation plus storage is then repeated with a repetition rate of 40 Hz.

$$|1\rangle_A = \sum_i c_i e^{i\delta_i t} e^{-ikz_i} |g \cdots e_i \cdots g\rangle \quad (2)$$

where z_i is the position of atom i (for simplicity, we only consider a single spatial mode defined by the direction of propagation of the input field), k is the wave-number of the light field, δ_i the detuning of the atom with respect to the laser frequency and the amplitudes c_i depend on the frequency and on the spatial position of the particular atom i . This collective state will rapidly de-phase since each term acquires an individual phase $e^{i\delta_i t}$ depending on the detuning. However, due to the periodic structure of the absorption profile, the collective state will be re-established after a pre-programmed time $2\pi/\Delta$, where Δ is the period of the spectral grating. This leads to a coherent photon-echo type re-emission in the forward spatial mode [11, 25, 26, 27]. Note that in our experiment the light field is stored as a collective excitation on the optical transition, contrary to all previous experiments at the single photon level, where collective excitations of spin states were used [5, 6, 7]. Conceptually, this is an important difference since in our case the light is simply absorbed in the prepared material, without any control field.

The solid state interface is implemented in an ensemble of Neodymium ions (Nd^{3+}) doped into a YVO_4 crystal [28]. The Nd^{3+} ions constitute an ensemble of inhomogeneously broadened atoms having a relevant level structure with two spin ground states $|g\rangle$ and $|aux\rangle$ and one excited state $|e\rangle$, as shown in Fig.1. Initially, the two ground states are equally populated for all frequencies over the inhomogeneous broadening. The preparation of the spectral grating is realized by frequency selective optical pumping from $|g\rangle$ to $|aux\rangle$ via the excited state $|e\rangle$ (see Fig.1 for an overview of the experiment). This is implemented with a Ramsey type interference using a train of coherent pairs of pulses [29] (see Fig. 1 and Methods). To store weak light fields, it is required that there is no population in the excited state, otherwise fluorescence will blur the signal. This is ensured by waiting long enough between the preparation and storage sequences, such that all atoms have returned to the ground states. As a result of the preparation sequence, a spectral grating is present in $|g\rangle$ before the storage begins, which decays with the population relaxation lifetime T_Z between the spin states ($T_Z = 6 \text{ ms}$ in our case).

In the first experiment, we demonstrate collective mapping of weak coherent states $|\alpha\rangle_L$ on the crystal. An example with $\bar{n} = 0.5$ is shown in Fig. 2 (See Methods

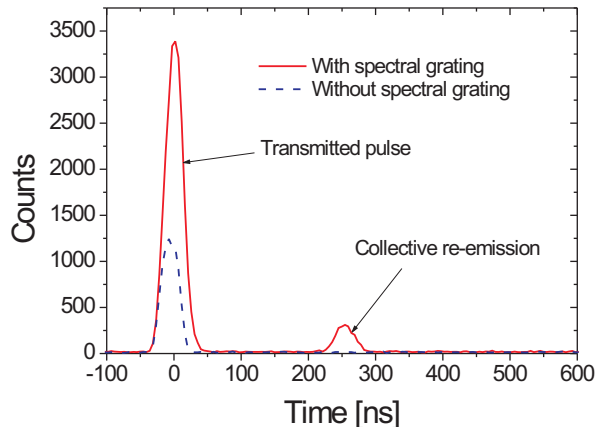


FIG. 2: Reversible mapping of a coherent state with $\bar{n} = 0.5$. The solid line corresponds to the case where a spectral grating is prepared with a periodicity of 4 MHz. The peak 250 ns after the transmitted input pulse corresponds to the collective retrieval after storage in the solid state medium. The dashed line corresponds to the case where the atomic medium is not prepared with a spectral grating. In that case, we only see the transmitted input pulse (about 2 percent of the incoming pulse is transmitted). The absorption of the input pulse is smaller when the spectral grating is prepared (about 5 percent of the light is transmitted)

for the estimation of \bar{n}). When the sample is prepared with a spectral grating having a periodicity of 4 MHz, we observe a strong emission at the expected storage time of 250 ns. About 0.5 percent of the incoming light is re-emitted in this signal. This is more than 4 orders of magnitude more than what would be expected from a non collective re-emission, taking into account that we collect a solid angle of $2 \cdot 10^{-4}$ and that the optical relaxation time is 3 orders of magnitude longer than the observed signal. This signal thus clearly arises from a collective re-emission, which demonstrates the collective and reversible mapping of a light field with less than one photon onto an large number of atoms in a solid. To further study the mapping process, we record the number of counts in the observed signal for different \bar{n} ranging from 0.2 to 2.7 (see Fig. 3 a). This shows that the mapping is linear and that very low photon numbers can still be mapped and retrieved. We also investigated the decay of storage efficiency with the storage time (see Fig. 3b).

The efficiency of the storage and retrieval and its decay as a function of storage time can be qualitatively understood using the theory of the AFC quantum memory [11]. In order to obtain high storage efficiencies for a given storage time, it is essential to create a spectral grating with narrow absorption peaks as compared to the spectral separation of the peaks, i.e. a high finesse grating [11]. In our experiment, however, the minimal width

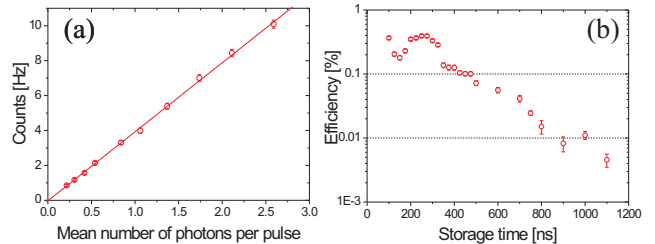


FIG. 3: (a) Number of detections in the collective output mode as a function of \bar{n} . (b) Efficiency as a function of the storage time for $\bar{n} = 2.7$. For small storage times (< 400 ns), an oscillation of the efficiency is clearly visible. This is a quantum beat due to the interaction of the electronic spin of the Nd^{3+} ion with the nuclear spin of the surrounding Vanadium ions (called super hyperfine interaction). For longer storage times, the decay is exponential with decay constant of 220 ns. This interaction also limits the minimal width of the absorption peaks.

of the absorption peak is of the order of 1-2 MHz, due to material properties (see Fig.3) and to the linewidth of our free-running laser. Hence the grating is close to a (low finesse) sinusoidal curve, which limits the storage efficiency and causes the observed decay of the efficiency vs storage time. Moreover, there is still a significant flat absorption background due to imperfect optical pumping in the present experiment. This background can be considered as a loss which strongly limits the observed storage efficiency. We emphasize however that these are not fundamental limitations of rare-earth materials. The preparation of narrow absorption lines with low absorption background has been demonstrated for several other rare-earth materials, such as $\text{Eu}:\text{Y}_2\text{SiO}_5$ [20], $\text{Pr}:\text{Y}_2\text{SiO}_5$ [21, 30] and $\text{Tm}:\text{YAG}$ [31]. Significantly higher storage efficiencies should be obtained in these materials [11]. Note also that the experiment described here implements a memory device with a fixed storage time. In order to allow for on-demand read-out of the stored field (as required for quantum repeaters) and storage times longer than that given by the spectral grating, the excitations in $|e\rangle$ can be transferred to a third ground state spin level $|s\rangle$. This transfer also enables in principle storage efficiencies close to unity [11].

So far we have considered the storage of weak light fields in a single temporal mode. However the use of spectral gratings also allows for the storage in multiple temporal modes as shown in [11]. The maximal number of modes that can be stored is given by the ratio of the storage time (determined by the spectral grating) to the duration of an individual mode. To illustrate this multi-mode property we store trains of four weak pulses with \bar{n} from 0.8 to 0.3 during 500 ns, as shown in Fig.4. It is important to note that the time ordering of the pulses is preserved during the storage, which results in the same storage efficiency for each mode. This is in contrast with

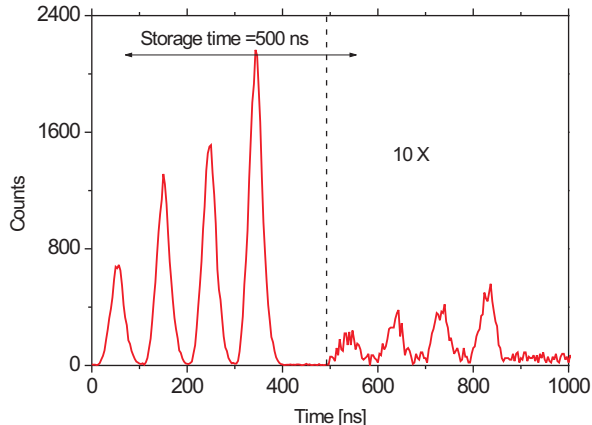


FIG. 4: Multimode light matter interface. The spectral grating is prepared for a storage time of 500 ns. The first four pulses are the transmitted pulses. After 500 ns, we can clearly see the collective re-emission of the four temporal modes. The signal to noise ratio is smaller than for the single mode case (fig. 2), due to the longer storage time of 500 ns (cf Fig.3 b). For clarity, the output signal part has been magnified by a factor of ten.

CRIB based quantum memories where the time ordering is reversed [16]. The number of stored modes for a given storage time can be improved by using shorter preparation pulses, resulting in larger bandwidth of the spectral grating. In this case, shorter pulses can be stored. In the present experiment, the shortest duration of pulses was set to about 20 ns (FWHM) by technical limitations. A great advantage of the AFC protocol is that the number of modes that one can store does not depend on the optical depth, contrary to EIT and CRIB [11].

For applications in quantum memories, it is crucial that the interface conserves the phase of the incoming pulses. To probe the coherence of the mapping process at the single photon level, we use a pair of weak pulses separated by a time $\tau = 100$ ns with a fixed relative phase Φ . This can be seen as a time bin qubit, which can be written as: $|\psi\rangle_L = |\alpha_t\rangle_L + e^{i\Phi}|\alpha_{t+\tau}\rangle_L$ where $|\alpha_t\rangle_L$ represents a weak coherent state at time t . The qubit is stored and thereafter analyzed directly in the memory using a method developed in Ref [22]. This method requires the implementation of partial read-outs at different times. This realizes a projection on a superposition basis, similarly to what can be done with a Mach-Zehnder interferometer [22]. If the time τ between the weak pulses matches the time between the two read-outs, the re-emission from the sample can be suppressed or enhanced depending on the phase difference between the two incoming pulses. The visibility of this interference is a measure of the coherence of the mapping process. The two partial read-outs are here achieved by preparing two super-imposed spectral gratings having different periods,

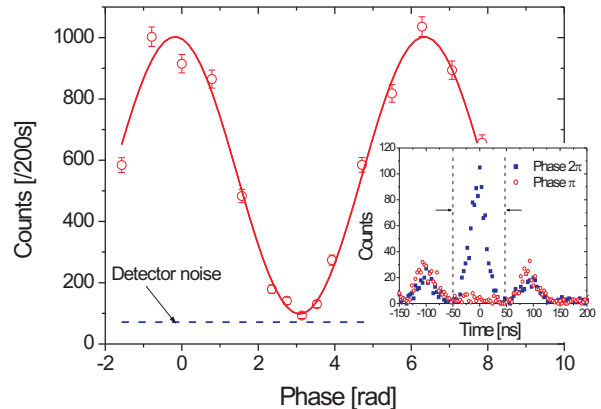


FIG. 5: Interference fringe. Time-bin qubits with different phases Φ are stored and analyzed using the interface. The analysis is performed by projecting the time-bin qubit on a fixed superposition basis, which here is achieved by two partial read-outs (see text for details). The inset shows the histogram of arrival times, where there is a constructive ($\Phi = 2\pi$) and destructive interference ($\Phi = \pi$) in the middle time bin. For this particular interference fringe, we obtain a raw visibility of 82%, or 95% when subtracting detector dark counts.

corresponding to storage times of 200 and 300 ns. An example of interference for $\bar{n} = 0.85$ is shown in Fig.5. Dark-counts subtracted visibilities above 95 % have been obtained for various \bar{n} between 0.4 and 1.7, which demonstrates the high coherence of the storage process, even at the single photon level. From these visibilities, one can infer conditional fidelities above 97 % for the storage of single photons [23]. This excellent phase preservation at the single photon level is obtained thanks to the collective enhancement effect [23] and to the almost complete suppression of background noise .

In conclusion, we have demonstrated the coherent and reversible mapping of a light field at the single photon level onto a solid. Our results show that the storage of single photons (Fock states) in multiple temporal modes in solids is possible. We have also demonstrated that the quantum coherence of the incident weak light fields is almost perfectly conserved during the storage. Solid state systems can therefore be considered as a promising alternative to atomic gases for photonic quantum storage. This line of research holds promise for the implementation of efficient long distance quantum networks.

Methods

The preparation of the spectral grating is realized by a series of pairs of pulses of area $\Theta < \pi/2$ resonant with the $|g\rangle \rightarrow |e\rangle$ transition. Each pair of pulses realizes a frequency selective coherent transfer of population from $|g\rangle$ to $|e\rangle$ [29]. This can be seen as a Ramsey type interference where the two light pulses play the role of beam splitters and the phase shift acquired in the excited state depends on the detuning of the atoms. The periodicity of the

created spectral grating is then given by the inverse of the time interval τ_s between the two pulses. The atoms in the excited state can decay to both ground states $|g\rangle$ and $|aux\rangle$ with a relaxation time $T_1=100\ \mu\text{s}$. The atoms that decay to $|aux\rangle$ are not affected by the preparation laser and remain in this state for a time of 6 ms [28]. The pulse sequence is then repeated 100 times with a time separation between the pairs of $15\ \mu\text{s}$, longer than the optical coherence time $T_2=7\ \mu\text{s}$. This allows for the build up of the spectral grating, with population storage in $|aux\rangle$.

To estimate the mean number of photons per pulse, we shift the laser out of resonance with the absorbing atoms and record the proportion of detections in the single photon counter (typically between 1% and 20%). By a careful measurement of the detection efficiency ($\eta_D=0.32$) and of the transmission efficiency from the input face of the cryostat to the detector (typically $\eta_t=0.2$), one can finally infer the mean number of photons in front of the cryostat, before the sample.

Acknowledgements We thank E. Cavalli and M. Bettinelli for kindly lending us the Nd:YVO₄ crystal. This work was supported by the Swiss NCCR Quantum Photonics and by the European Commission under the Integrated Project Qubit Applications (QAP).

REFERENCES

-
- [1] Briegel H.-J., Dür W., Cirac J. I., and Zoller. P. Quantum repeaters: The role of imperfect local operations in quantum communication. *Phys. Rev. Lett.*, **81**, 5932 (1998).
- [2] L.-M. Duan, M. D. Lukin, J. I. Cirac, and P. Zoller. Long-distance quantum communication with atomic ensembles and linear optics. *Nature*, **414**, 413 (2001).
- [3] C. Simon, H. de Riedmatten, M. Afzelius, N. Sangouard, H. Zbinden, and N. Gisin. Quantum repeaters with photon pair sources and multimode memories. *Phys. Rev. Lett.* **98**, 190503 (2007).
- [4] B. Julsgaard, J. Sherson, J. I. Cirac, J. Fiurášek, and E. S. Polzik. Experimental demonstration of quantum memory for light. *Nature* **432**, 482 (2004).
- [5] T. Chanelière, *et al* Storage and retrieval of single photons transmitted between remote quantum memories. *Nature* **438**, 833(2005).
- [6] M. D. Eisaman *et al* Electromagnetically induced transparency with tunable single-photon pulses. *Nature* **438**, 837(2005).
- [7] C. W. Chou, H. de Riedmatten, D. Felinto, S. V. Polyakov, S. J. van Enk, and H. J. Kimble. Measurement-induced entanglement for excitation stored in remote atomic ensembles. *Nature*, **438**, 828(2005)
- [8] K. Honda *et al*. Storage and retrieval of a squeezed vacuum. *Phys. Rev. Lett.* **100**, 093601 (2008).
- [9] J. Appel, E. Figueroa, D. Korystov, M. Lobino, and A. I. Lvovsky. Quantum memory for squeezed light. *Phys. Rev. Lett.* **100**, 093602 (2008).
- [10] A. D. Boozer, A. Boca, R. Miller, T. E. Northup, and H. J. Kimble. Reversible state transfer between light and a single trapped atom. *Phys. Rev. Lett.* **98**, 193601 (2007).
- [11] M. Afzelius, C. Simon, H. de Riedmatten, and N. Gisin. Multimode quantum memory based on atomic frequency combs. *arXiv:0805.4164*, 2008.
- [12] M. Fleischhauer and M. D. Lukin. Dark-state polaritons in electromagnetically induced transparency. *Phys. Rev. Lett.* **84**, 5094 (2000).
- [13] J. Nunn *et al* Mapping broadband single-photon wave packets into an atomic memory. *Phys. Rev. A* **75**, 011401 (2007).
- [14] S. A. Moiseev and S. Kröll. Complete reconstruction of the quantum state of a single-photon wave packet absorbed by a doppler-broadened transition. *Phys. Rev. Lett.* **87**, 173601 (2001).
- [15] M. Nilsson and S. Kröll. Solid state quantum memory using complete absorption and re-emission of photons by tailored and externally controlled inhomogeneous absorption profiles. *Optics Communications* **247**,393 (2005).
- [16] B. Kraus, W. Tittel, N. Gisin, M. Nilsson, S. Kröll, and J. I. Cirac. Quantum memory for nonstationary light fields based on controlled reversible inhomogeneous broadening. *Phys. Rev. A* **73**, 020302 (2006).
- [17] T. Böttger, C. W. Thiel, Y. Sun, and R. L. Cone. Optical decoherence and spectral diffusion at $1.5\ \mu\text{m}$ in Er³⁺:Y₂SiO₅ versus magnetic field, temperature, and Er³⁺ concentration. *Phys. Rev. B* **73**, 075101 (2006).
- [18] E. Fraval, M. J. Sellars, and J. J. Longdell. Dynamic decoherence control of a solid-state nuclear-quadrupole qubit. *Phys. Rev. Lett.* **95**, 030506 (2005).
- [19] J. J. Longdell, E. Fraval, M. J. Sellars, and N. B. Manson. Stopped light with storage times greater than one second using electromagnetically induced transparency in a solid. *Phys. Rev. Lett.* **95**,063601 (2005).
- [20] A. L. Alexander, J. J. Longdell, M. J. Sellars, and N. B. Manson. Photon echoes produced by switching electric fields. *Phys. Rev. Lett.* **96**, 043602 (2006).
- [21] G. Hétet, J. J. Longdell, A. L. Alexander, P. K. Lam, and M. J. Sellars. Electro-optic quantum memory for light using two-level atoms. *Phys. Rev. Lett.* **100**, 023601 (2008).
- [22] M. U. Staudt *et al* Fidelity of an optical memory based on stimulated photon echoes. *Phys. Rev. Lett.* **98**, 113601 (2007).
- [23] M. U. Staudt *et al* Interference of multimode photon echoes generated in spatially separated solid-state atomic ensembles. *Phys. Rev. Lett.* **99**, 173602 (2007).
- [24] N. Ohlsson, M. Nilsson, and S. Kröll. Experimental investigation of delayed self-interference for single photons. *Phys. Rev. A* **68**, 063812(2003).
- [25] T. Mossberg, A. Flusberg, R. Kachru, and S. R. Hartmann. Total scattering cross section for Na on He measured by stimulated photon echoes. *Phys. Rev. Lett.* **42**, 1665 (1979).
- [26] N. W. Carlson, Y. S. Bai, W. R. Babbitt, and T. W. Mossberg. Temporally programmed free-induction decay. *Phys. Rev. A*, **30**, 1572 (1984).
- [27] M. Mitsunaga, R. Yano, and N. Uesugi. Spectrally programmed stimulated photon echo. *Opt. Lett.*, **16**, 264 (1991).
- [28] S. R. Hastings-Simon *et al* Spectral hole burning spectroscopy in Nd³⁺: YVO₄. *Phys.Rev.B*, **77**, 125111 (2008).
- [29] W. H. Hesselink and D. A. Wiersma. Picosecond photon echoes stimulated from an accumulated grating. *Phys. Rev. Lett.*, **43**, 1991 (1979).
- [30] L. Rippe, B. Julsgaard, A. Walther, Yan Ying, and S. Kröll. Experimental quantum-state tomography of a solid-state qubit. *Phys. Rev. A*, **77**, 022307 (2008).
- [31] F. de Sèze, V. Lavielle, I. Lorgeré, and J. L. Le Gouët. Chirped pulse generation of a narrow absorption line in a Tm³⁺:YAG crystal. *Optics Communications*, **223**, 321

(2003).